Journal of Alloys and Compounds 495 (2010) 97–103

Contents lists available at ScienceDirect

Journal of Alloys and Compounds

journal homepage: www.elsevier.com/locate/jallcom

Study of Nd:YAG laser annealing of electroless Ni–P film on spiegel-iron plate by Taguchi method and grey system theory

W.L. Liu [a], W.T. Chien [b], M.H. Jiang [b], W.J. Chen [c,*]

[a] Department of Materials Science and Engineering, National Formosa University, 64, Wunhua Road, Huwei, Yunlin 632, Taiwan, ROC
[b] Department of Mechanical Engineering, National Pingtung University of Science and Technology, 1, Shuehfu Road, Neipu, Pingtung 912, Taiwan, ROC
[c] Graduate School of Materials Science, National Yunlin University of Science and Technology, 123 University Road, Section 3, Douliou, Yunlin 64002, Taiwan, ROC

ARTICLE INFO

Article history:
Received 19 August 2009
Received in revised form 16 January 2010
Accepted 20 January 2010
Available online 25 January 2010

Keywords:
Laser annealing
Electroless Ni–P film
Taguchi method
Grey system theory

ABSTRACT

An electroless Ni–P film was first deposited on a spiegel-iron plate and then annealed by an Nd:YAG pulsed wave laser. In order to obtain the optimal laser annealing parameters for maximizing the hardness and minimizing the surface roughness of electroless Ni–P films, the Taguchi method and grey system theory were used to analyze the experimental data. The electroless Ni–P film was also characterized by scanning electron microscopy for the morphology, and transmission electron microscopy for the microstructure and crystal structure. The results showed that the hardness and the surface roughness of electroless Ni–P films can be, at the same time, improved to 50.8% and 68%, respectively, by the laser annealing with the optimal parameters.

1. Introduction

The electroless Ni–P films possess many advantages such as easy operation, low cost compared to the vacuum deposition process, uniform thickness, anti-wear, and corrosion-resistance, so they have been applied to a wide variety of fields, for examples, aviation, automobile, food, electronic, chemical, mechanical, and other industries. The properties of electroless Ni–P films are chiefly determined by the microstructure, composition, and crystal structure of films, and can be controlled by adjusting the plating bath composition, operating condition, and annealing treatment [1–4].

Lu et al. [5] showed that when the annealing temperature for electroless Ni–P films with P element ranging from 7% to 13% is increased, the hardness and the wear resistance all go through a maximum value, but these two maxima do not occur at the same annealing temperature. Osaka et al. [6] confirmed that the saturation magnetization and the reciprocal of resistivity of electroless Ni–P films are proportional to the amount of the residual Ni, which means the surplus Ni after Ni–P formation, after sufficient heat treatment. It was found that increasing the phosphorus content would change the structure from crystalline to amorphous and decrease the thermal stability of electroless Ni–P film [7]. It was shown that high hardness can be obtained when phosphorus content and heat treatment are proper and this technology can be used in repairing and manufacturing moulds. The electroless Ni–P films with 11.1–13.1% P were shown to be amorphous and better corrosion-resistant than microcrystalline structure [8].

Most of the electroless Ni–P films were annealed by conventional furnaces [9–12], and a few by laser [13–15]. In the conventional annealing process, the film and the substrate both are heated and cooled so that relatively much energy is needed and the interdiffusion and reaction between Ni–P film and substrate may take place. In the laser annealing process, the surface would undergo rapid melting and subsequent rapid self-quenching cooling by the bulk substrate so that a structure with ultra-fine grains or precipitates could be produced on the surface layer due to the larger liquid undercooling. Therefore, material surface processing with laser has attracted increasing attentions and has been widely utilized to improve the surface roughness and wear resistance [16–18].

Taguchi et al. [19] developed a method for robust design between 1950 and 1960. The Taguchi method is very suitable for the study of thin film coatings, because the properties of thin film coatings are affected by a lot of deposition parameters which can be optimized by the Taguchi method with less labor, time, cost, and better quality. The Taguchi method has been applied to various thin film coatings, such as copper deposition on printed circuit boards [20], nickel coated protein chips by electroplating technology [21], TiN coatings on cutting tools by cathodic arc physical vapor deposition [22], multiple-criteria problems of VLSI manufacturing process [23], nickel chrome sputtered to Al_2O_3 [24], etc. In this work, an electroless Ni–P film was fist deposited on a spiegel-

* Corresponding author. Fax: +886 5 531 2194.
E-mail address: chenwjau@yuntech.edu.tw (W.J. Chen).

0925-8388/$ – see front matter © 2010 Elsevier B.V. All rights reserved.
doi:10.1016/j.jallcom.2010.01.094

iron plate and then annealed by an Nd:YAG pulsed wave laser. The Taguchi method and grey system theory were used to analyze the experimental results in order to obtain the optimal laser annealing parameters for maximizing the hardness and minimizing the surface roughness of electroless Ni–P films on spiegel-iron plate.

2. Experimental

2.1. Preparation of electroless Ni–P films

A spiegel-iron plate with 0.5 mm in thickness was used as the substrate for the electroless Ni–P deposition. The spiegel-iron is one kind of white cast iron containing Mn, which can be used as tie rod, gear, valve, and other resistance castings. In this work an electroless NiP film was deposited on the spiegel-iron plate to improve the surface roughness and the hardness of the plate. The bath composition and operation condition for the electroless Ni–P deposition were shown in Table 1 in which the nickel sulfate, sodium succinite, lead nitrate, and sodium hypophosphite were taken as the nickel source, complexing agent, stabilizer, and reducing agent, respectively. The deposition time is 20 min so that an electroless Ni–P film about 0.65 μm in thickness can be formed on the spiegel-iron plate.

2.2. Annealing of electroless Ni–P films

An Nd:YAG pulsed wave laser (KLS246-102) was used as the heat source for the annealing of electroless Ni–P films. The Nd:YAG pulsed wave laser has a wavelength of 1.064 μm and a beam diameter of 2 mm. The annealing condition was shown in Table 2. The parameters of annealing process consist of atmosphere (factor *A*), laser peak power (factor *B*), pulse duration time (factor *C*), pulse frequency (factor *D*), height of laser beam focus above the sample surface (factor *E*), scanning speed of laser beam (factor *F*), separation distance between scanning lines (factor *G*), and pumping frequency in laser resonator (factor *H*). Excepting factor *A* with two levels, there are three levels for the other factors. These factors and their levels were so selected based on the result of the prior experiments in which the electroless films after annealing did not crack.

2.3. Analysis based on Taguchi method and grey system theory

In order to find the optimal laser annealing parameters for maximizing the hardness and minimizing the surface roughness of electroless Ni–P films, an orthogonal array of L_{18} ($2^1 \times 3^7$) was taken for the design of various laser annealings of electroless Ni–P films and there are 18 experiments in total. The experimental results, i.e. hardness and roughness of electroless Ni–P films, were first transformed into signal-noise ratio and then treated by using analysis of mean (ANOM) and analysis of variance (ANOVA). The optimal parameters of laser annealing respectively for maximizing the hardness and minimizing the roughness of electroless Ni–P films can be finally obtained. The signal-noise ratios of the hardness and the roughness of electroless Ni–P films can be further normalized and then treated by using grey relational analysis (GRA) [25]. The optimal parameters of laser annealing simultaneously for maximizing the hardness and minimizing the roughness of electroless Ni–P films can be obtained.

2.4. Characterization of electroless Ni–P films

The electroless Ni–P films were characterized by a scanning electron microscope (SEM) (JEOL JEM6380) for the surface morphology, a transmission electron microscope (TEM) (JEOL 2010EX) for the microstructure and crystal structure, and a nano-indenter system equipped with an atom force microscope (Digital Instruments CP-II Scanning probe Microscope) for the hardness and the roughness.

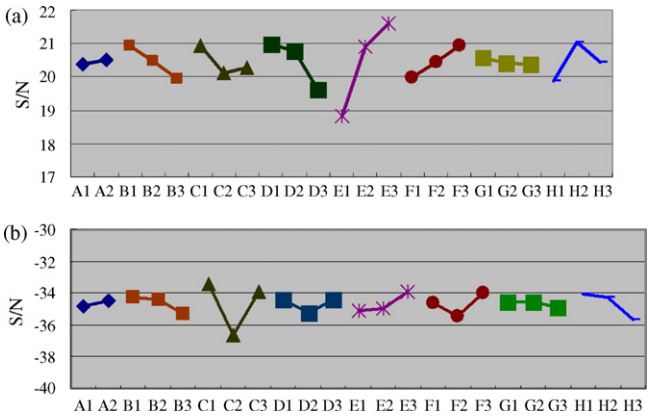

Fig. 1. The diagram of response of signal-noise ratios S/N, for (a) the hardness, and (b) the surface roughness of electroless Ni–P films after various laser annealings.

3. Results and discussion

3.1. Optimization of laser annealing parameters for the hardness of electroless Ni–P films

The film hardness and its corresponding signal-noise ratio (S/N), are shown in Table 3(a) for the 18 experiments. Each value of film hardness is the average of five measurements and the signal-noise ratio is calculated by the formula: $S/N = -10 \log\left(1/n\sum_{i=1}^{n} 1/y_i^2\right)$ (db), where y_i is the film hardness, $n = 5$, and db is the unit, decibel. The largest hardness and smallest hardness are 13.3 Gpa of the 13th experiment and 7.732 Gpa of the 14th experiment, respectively.

Table 4(a) shows the response of signal-noise ratio (S/N), for each control factor at a given level and its corresponding diagram is shown in Fig. 1(a). Each value in Table 4(a) is calculated by the formula: $M_{f,l} = 1/n\sum_{l=1}^{n}(S/N)_{f,1}$, where $M_{f,l}$ is the average of signal-noise ratio (S/N) for each control factor at a given level, and n is the number of the given level for a control factor among the 18 experiments. From Table 4(a) it is obvious that the factor *E* (height of laser focus above the film surface) has the largest effect on the film hardness.

The analysis of variance (ANOVA) for the signal-noise ratio of the film hardness is shown in Table 5(a) in which SS, DOF, Var, and *F* denote the sum of squares of variance, degree of freedom, variance, and *F*-ratio, respectively. The SS of *A* factor (atmosphere) and *G* factor (separation distance between scanning lines) are so small that they are pooled as experiment error. The percentage contribution of error is only 3.21% which demonstrates the design for the 18 experiments is suitable and reasonable for the laser annealing of electroless Ni–P films.

Table 1
The bath composition and operation condition for the electroless Ni–P deposition.

Bath composition and operation parameters	$NiSO_4{\cdot}6H_2O$	$Na_2C_4H_4O_4{\cdot}6H_2O$	$Pb(NO_3)_2$	$NaH_2PO_2{\cdot}H_2O$	pH	Temperature	Deposition time
Specification	20 g/l	16 g/l	4 ppm	27 g/l	4.5	70 °C	20 min

Table 2
The control factors and their levels of laser annealing for the electroless Ni–P films.

Symbol	*A*	*B*	*C*	*D*	*E*	*F*	*G*	*H*
Laser annealing parameters	Atmosphere	Peak power (W)	Pulse duration time (ms)	Pulse frequency (Hz)	Focus height (mm)	Scanning speed (mm/S)	Separation between scanning lines (mm)	Pumping frequency in laser resonator (Hz)
Level 1	Ar	800	0.44	120	11	8	0.3	30
Level 2	N_2	750	0.42	110	10.5	6	0.25	20
Level 3		700	0.4	100	10	4	0.2	10

Table 3
(a) The hardness and its corresponding signal-noise ratio (S/N), and (b) the surface roughness and its corresponding signal-noise ratio (S/N), of the electroless Ni–P films after various laser annealings.

Exp.	1	2	3	4	5	6	7	8	9	10	11	12	13	14	15	16	17	18
(a)																		
Ave.	9.39	12.63	12.61	12.45	12.23	7.90	9.31	7.85	12.80	11.43	10.69	11.51	13.30	7.73	11.38	11.91	11.22	8.01
S/N	19.39	21.90	21.53	21.87	21.69	17.95	19.36	17.89	21.92	21.12	20.53	21.18	22.45	17.73	21.12	21.48	20.97	18.04
(b)																		
Ave.	42.53	75.22	46.01	58.07	55.54	46.14	59.43	72.44	50.51	39.29	58.94	56.37	43.1	51.04	41.1	42.65	69.22	60.62
S/N	−32.59	−37.53	−33.26	−35.29	−34.91	−33.29	−35.49	−37.21	−34.07	−31.89	−35.41	−35.02	−32.69	−38.17	−32.28	−32.60	−36.81	−35.66

Table 4
Response of signal-noise ratio, S/N, for (a) the hardness and (b) the surface roughness of electroless Ni–P films after various laser annealings.

Factor	*A*	*B*	*C*	*D*	*E*	*F*	*G*	*H*
(a)								
Level 1	20.39	20.94	20.95	20.97	18.83	19.97	20.57	19.87
Level 2	20.51	20.47	20.12	20.77	20.91	20.43	20.40	21.04
Level 3		19.94	20.29	19.62	21.61	20.95	20.39	20.44
Effect	0.12	1.00	0.83	1.35	2.78	0.98	0.18	1.16
Rank	8	4	6	2	1	5	7	3
(b)								
Level 1	−34.85	−34.28	−33.42	−34.41	−35.10	−34.60	−34.56	−34.09
Level 2	−34.50	−34.44	−36.67	−35.22	−34.99	−35.43	−34.55	−34.26
Level 3		−35.30	−33.93	−34.40	−33.94	−33.99	−34.92	−35.67
Effect	0.34	1.02	3.25	0.81	1.16	1.44	0.37	1.59
Rank	8	5	1	6	4	3	7	2

It can be seen from Table 4(a) and Fig. 1(a) that the optimal annealing parameters for maximizing the film hardness are *A*2 (atmosphere of N_2), *B*1 (laser peak power of 800 W), *C*1 (pulse duration time of 0.44 ms), *D*1 (laser pulse frequency of 120 Hz), *E*3 (laser focus height of 10 mm), *F*3 (laser scanning speed of 4 mm/s), *G*1 (scanning line separation of 0.3 mm), and *H*2 (pumping frequency of 20 Hz). The confirmation experiment with these optimal parameters was performed and the hardness for the confirmation experiment is 13.41 Gpa which is larger than 13.30 Gpa, the largest of the 18 experiments shown in Table 3(a). The hardness of the electroless Ni–P film after laser annealing with the optimal parameters is increased to 13.41 Gpa from 7.75 Gpa of the hardness of as-deposited film, in other words, the hardness of electroless Ni–P film can be promoted 73% by the laser annealing with optimal parameters.

3.2. Optimization of laser annealing parameters for the surface roughness of electroless Ni–P films

The surface roughness of electroless Ni–P films and its corresponding signal-noise ratio (S/N) are shown in Table 3(b) for the 18 experiments. Each value of surface roughness is the average of three measurements and the signal-noise ratio (S/N) is calculated by the formula: $S/N = -10\log\left(1/n\sum_{i=1}^{n}1/y_i^2\right)$ (db), where y_i is the surface roughness, $n = 3$. The largest surface roughness and smallest surface roughness are 81.04 nm of the 14th experiment and 32.29 nm of the 10th experiment, respectively.

Table 4 (b) shows the response of signal-noise ratio (S/N) for each control factor at a given level and its corresponding diagram is shown in Fig. 1(b). The result of Table 4(b) shows that the factor

Table 5
Analysis of variance (ANOVA) of signal-noise ratio (S/N), for (a) hardness and (b) the surface roughness of the electroless Ni–P films after various annealings.

Factor	SS	DOF	Var	*F*	Contribution
(a)					
A			Pooled		
B	3.010603	2	1.505302	18.04749	6.44%
C	2.288328	2	1.144164	13.71771	4.81%
D	6.4048446	2	3.202422	38.39476	14.13%
E	25.081701	2	12.54085	150.3558	56.44%
F	2.885678	2	1.442839	17.29861	6.16%
G			Pooled		
H	4.0573544	2	2.028677	24.32239	8.81%
Error	0.417039	5	0.083408		3.21%
Total	44.145548	17			
(b)					
A	0.531109	1	0.531109	6.88752385	0.70%
B	3.637944	2	1.818972	23.58878034	5.41%
C	36.65947	2	18.32974	237.7036035	56.66%
D	2.630757	2	1.315379	17.05808781	3.84%
E	4.925502	2	2.462751	31.93843434	7.41%
F	6.292032	2	3.146016	40.798188257	9.53%
G	0.533334	2	0.266667	3.458188257	0.59%
H	9.067424	2	4.533712	58.79406144	13.83%
Error	0.154223	2	0.077112		2.03%
Total	64.4318	17			

Table 6
(a) Normalization of signal-noise ratio (S/N) of film hardness and surface roughness and (b) series difference between hardness, roughness and reference series.

No. of experiment	Hardness reference series 1	Roughness reference series 1
(a)		
1	0.351551	0.888559
2	0.882899	0.102971
3	0.80462	0.781502
4	0.877374	0.459339
5	0.839139	0.519419
6	0.045778	0.777728
7	0.344376	0.427469
8	0.032648	0.154223
9	0.886552	0.65304
10	0.716903	1
11	0.591998	0.440003
12	0.730664	0.501379
13	1	0.872076
14	0	0
15	0.717881	0.93802
16	0.793052	0.886426
17	0.685206	0.217394
18	0.064779	0.400787

Exp.	Difference of hardness	Difference of roughness
(b)		
1	0.648449	0.11144124
2	0.117101	0.89702914
3	0.19538	0.2184981
4	0.122626	0.54066075
5	0.160861	0.48058072
6	0.954222	0.22227236
7	0.655624	0.57253119
8	0.967352	0.84577738
9	0.113448	0.34695988
10	0.283097	0
11	0.408002	0.55999696
12	0.269336	0.49862061
13	0	0.12792437
14	1	1
15	0.282119	0.06198001
16	0.206948	0.11357394
17	0.314794	0.7826061
18	0.935221	0.59921341

C (laser pulse duration time) has the largest effect on the surface roughness of electroless Ni–P films.

The analysis of variance (ANOVA) of signal-noise ratio (S/N) for the surface roughness is shown in Table 5(b). The percentage contribution of error is only 2.03% which demonstrates no any important factor has been neglected in the experiment design. The

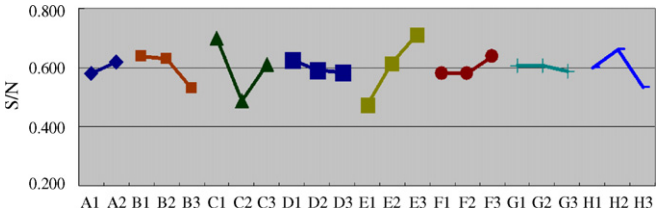

Fig. 2. The diagram of response of grey relational grade value for the hardness and the surface roughness of electroless Ni–P films.

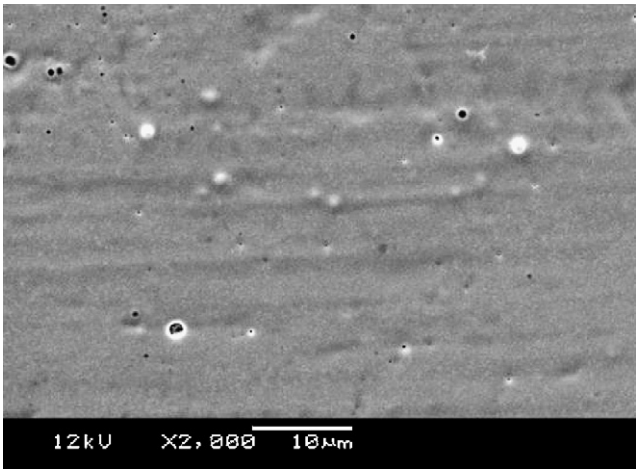

Fig. 3. SEM view of the surface morphology of electroless Ni–P film after annealing in confirmation experiment.

C factor (laser pulse duration time) has the largest percentage of 56.66% which is consistent with the result of signal-noise ratio (S/N) response.

It can be seen from Table 4(b) and Fig. 1(b) that the optimal annealing parameters for the surface roughness of electroless Ni–P films are *A*2 (annealing atmosphere of N_2), *B*1 (laser peak power of 800 W), *C*1 (laser pulse duration time of 0.44 ms), *D*3 (laser scanning speed of 4 mm/s), *G*2 (laser scanning line separation of 0.2 mm), and *H*1 (pumping frequency of 30 Hz). The confirmation experiment with these optimal parameters was carried out and the surface roughness of electroless films for the confirmation experiment is 30.84 nm which is smaller than 39.29 nm, the smallest of the 18 experiments shown in Table 3(b). The surface roughness of electro-

Table 7
Grey relational coefficient value, grey relational grade value and order of grey relational grade value for the hardness and surface roughness of electroless Ni–P films.

No. of experiments	Grey relational coefficient value of hardness	Grey relational coefficient value of roughness	Grey relational grade value	Order of grey relational grade value
1	0.43537	0.81774	0.626555	9
2	0.81024	0.357902	0.584071	10
3	0.719032	0.695896	0.707464	5
4	0.803051	0.480464	0.641757	7
5	0.756588	0.509902	0.633245	8
6	0.343826	0.69226	0.518043	12
7	0.432667	0.466187	0.449427	15
8	0.34075	0.371532	0.356141	17
9	0.815065	0.590347	0.702706	6
10	0.638491	1	0.819245	2
11	0.55066	0.471699	0.51118	13
12	0.649911	0.500691	0.575301	11
13	1	0.796274	0.898137	1
14	0.333333	0.333333	0.333333	18
15	0.639289	0.889711	0.7645	3
16	0.707266	0.814898	0.761082	4
17	0.613652	0.389831	0.501742	14
18	0.348378	0.454871	0.401625	16

Table 8
Response of grey relational grade for the hardness and surface roughness of electroless Ni–P films.

Factor	*A*	*B*	*C*	*D*	*E*	*F*	*G*	*H*
Level 1	0.580	0.637	0.699	0.625	0.473	0.579	0.605	0.600
Level 2	0.618	0.632	0.487	0.590	0.614	0.580	0.606	0.663
Level 3	*X*	0.529	0.612	0.583	0.710	0.638	0.586	0.535
Effect	0.039	0.109	0.213	0.042	0.237	0.058	0.020	0.128
Rank	7	4	2	6	1	5	8	3

less Ni–P films after laser annealing with the optimal parameters is decreased to 30.84 nm from 110.5 nm of the surface roughness of the as-deposited electroless Ni–P film. In other words, the surface roughness of electroless Ni–P film can be improved 72% by the laser annealing with optimal parameters.

3.3. Optimization of laser annealing parameters simultaneously for the hardness and the surface roughness of electroless Ni–P films

The optimal annealing parameters are *A*2, *B*1, *C*1, *D*3, *E*3, *F*3, *G*1, and *H*2 for the hardness of electroless Ni–P film, but are *A*2, *B*1, *C*1, *D*3, *E*3, *F*3, *G*2, and *H*1 for the surface roughness Ni–P films. For obtaining the optimal annealing parameters simultaneously for the hardness and surface roughness of electroless Ni films, the signal-noise ratio (S/N) of hardness and surface roughness in Table 3(a) and (b) was used for the grey relational analysis (GRA). Table 6(a) shows the normalization of signal-noise ratio (S/N) of film hardness and surface roughness of the electroless Ni–P films in which each normalization value is obtained by the formula:

$$Xi^*(k) = \frac{Xi(k) - \min[Xi(k)]}{\max[Xi(k)] - \min[Xi(k)]},$$

where $Xi^*(k)$, $Xi(k)$, $\max[Xi(k)]$, and $\min[Xi(k)]$ are normalized value, value in series k, maximum and minimum in series K, respectively. The value in reference series is taken as 1. Table 6(b) shows the difference between hardness series and reference series, and the difference between roughness series and reference series, respectively, in which each difference value is obtained by the formula: $\Delta oi(k) = |Xi^*(k) - Xo^*(k)|$, where $\Delta oi(k)$, $Xi^*(k)$, and $Xo^*(k)$, are the difference value, normalized value of series k, and normalized value of reference series, respectively. Table 7 shows the grey relational coefficient value of film hardness (γ_{hardness}) and the grey relational coefficient value of surface roughness ($\gamma_{\text{roughness}}$), the grey relational grade value (γ_T), and the order of grey relational grade, in which the grey relational coefficient value is obtained by the formula: $\gamma(k) = (\Delta_{\min} + \zeta\,\Delta_{\max})/(\Delta oi(k) + \zeta\,\Delta_{\max})$, where $\gamma(k)$ is the

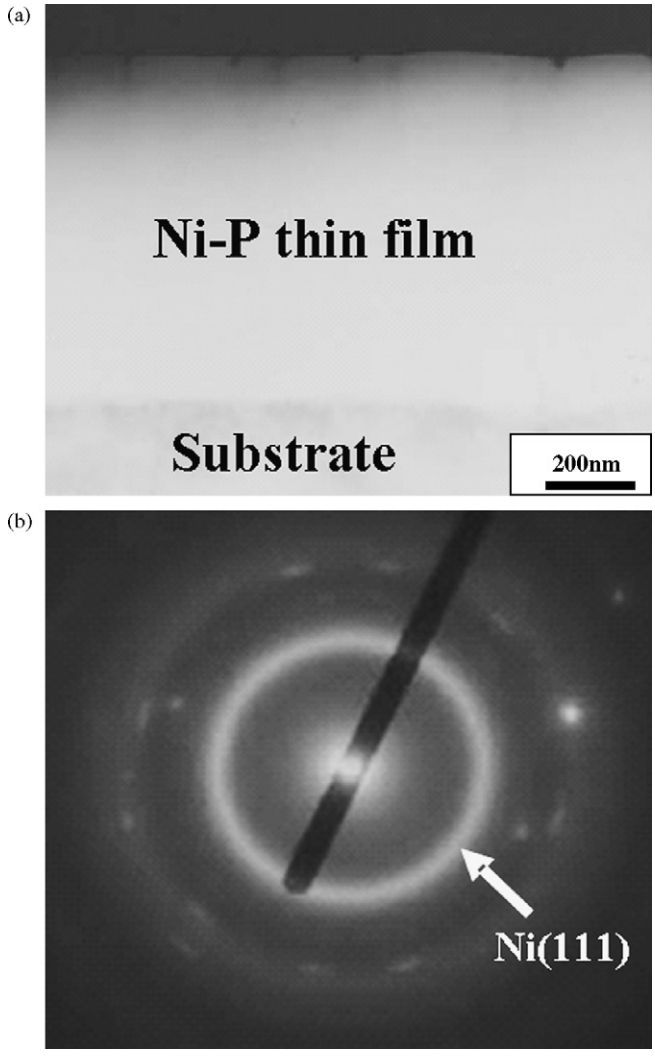

Fig. 4. (a) TEM cross-sectional view and (b) TEM selected area diffraction pattern of as-deposited Ni–P films.

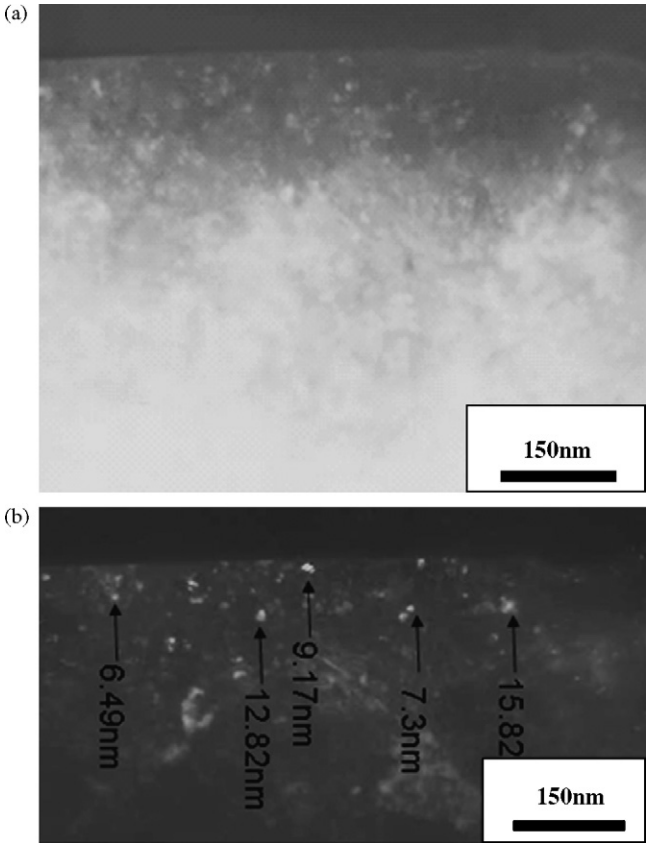

Fig. 5. (a) TEM cross-sectional bright field (BF) image, and (b) dark field (DF) image of a sample after laser annealing.

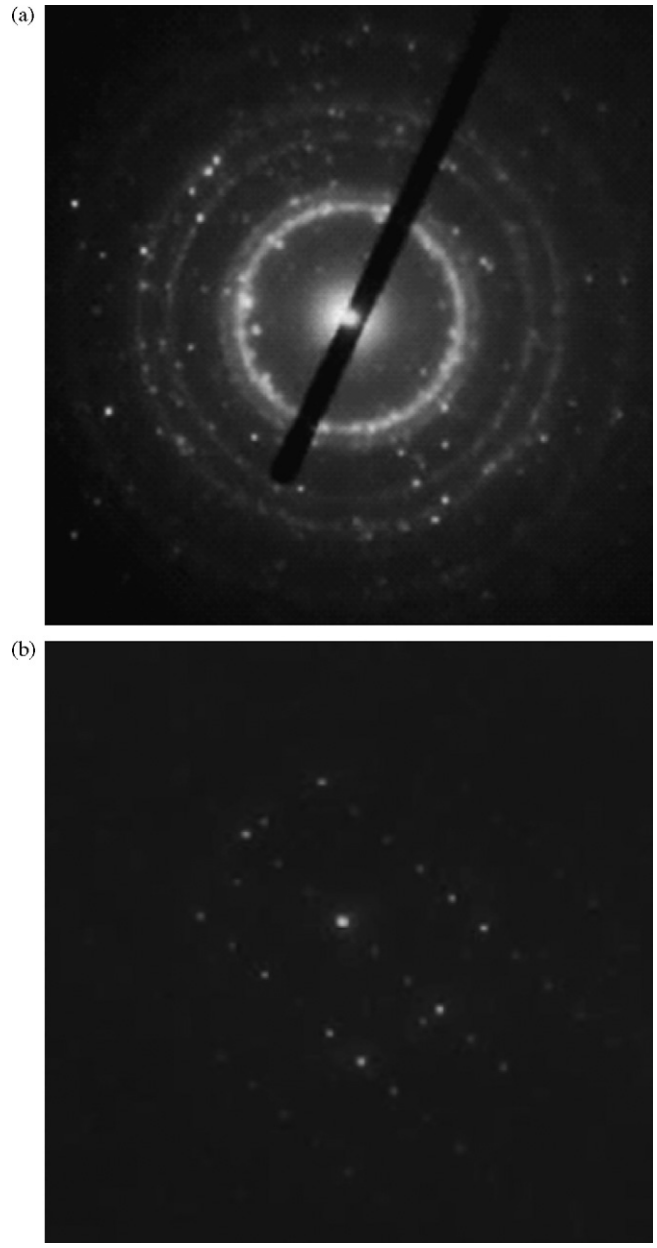

Fig. 6. TEM selected area diffraction pattern of a sample after laser annealing.

grey relational coefficient value of hardness and roughness, Δ_{min} and Δ_{max} are the minimum and the maximum of difference value in Table 6(b), ζ is the distinguishing coefficient and is taken as 1/2 here. The grey relational grade value (γ_T) is obtained by the formula: $\gamma_T = \sum_{k=1}^{n} B_k \gamma(K)$, where B_k is the weighing factor for $\gamma(k)$ and is taken as 1/2 here.

The response of grey relational grade value for hardness and surface roughness of electroless Ni–P films is shown in Table 8 and its corresponding diagram is shown in Fig. 2. It can be seen from Table 8 and Fig. 2 that the optimal annealing parameters simultaneously for the hardness and surface roughness of electroless Ni–P films are *A*2 (annealing atmosphere of N_2), *B*1 (laser pulse peak power of 800 W), *C*1 (laser pulse duration time of 0.44 ms), *D*1 (laser pulse frequency of 120 Hz), *E*3 (laser focus height of 10 mm), *F*3 (laser scanning speed of 4 mm/s), *G*2 (laser scanning line separation of 0.21 mm), and *H*2 (pumping frequency of 20 Hz). The confirmation experiment with these optimal parameters was carried out and the hardness and the surface roughness of electroless Ni–P films are 11.69 Gpa and 35.22 nm, respectively. After the electroless Ni–P film is annealed with these optimal parameters its hardness is increased to 11.69 Gpa from 7.75 Gpa of the as-deposited film and its surface roughness is decreased to 35.22 nm from 110.05 nm of the as-deposited film, in other words, the hardness and the surface roughness of the electroless Ni–P film can be at the same time improved 50.8% and 68%, respectively, by the laser annealing with these optimal parameters.

3.4. The microstructure and crystal structure of electroless Ni–P films

Fig. 3 shows a typical SEM view of the surface morphology of an electroless Ni–P film. There are some pinholes and inclusions dispersed on the film surface. These inclusions have an average composition of 33 at.% C, 2 at.% O, 13 at.% P, 4 at.% Fe, and 48 at.% Ni. The surface roughness of the film is 30.84 nm which is smaller than 110.5 nm of the surface roughness of the as-deposited electroless Ni–P film due to the laser annealing treatment. In the annealing process, the Ni–P film could melt very quickly and then solidify when the Ni–P film is melted, its surface could be smoothed due to the liquid surface tension and has a relatively small surface roughness. Fig. 4(a) shows the TEM cross-sectional view of an as-deposited Ni–P film. The Ni–P film is about 670 nm in thickness and looks homogeneous in microstructure. The TEM selected area diffraction pattern of an as-deposited Ni–P film is shown in Fig. 4(b). The diffusive rings in diffraction pattern show the as-deposited Ni–P film is amorphous. The TEM cross-sectional views of an electroless Ni–P film after laser annealing are shown in Fig. 5(a) and (b). The film is not homogeneous in microstructure. There are many nanosized particles dispersed in the film. These nanosized particles are mostly Ni_3P confirmed by the TEM selected area diffraction pattern shown in Fig. 6(a) and (b). These nanosized particles were formed in the process of laser annealing and are the key factor for the hardening of electroless Ni films. The size of Ni_3P particles is only about 10 nm. This means that the time for the growth of Ni_3P particles is very short due to the large cooling rate.

4. Conclusion

An Nd:YAG laser was used to anneal the electroless Ni–P film deposited on the substrate of spiegel-iron for increasing the hardness and decreasing the surface roughness of Ni–P film. For only maximizing the film hardness the two most important laser annealing parameters are laser focus height and laser pulse frequency. The hardness of electroless Ni–P film after laser annealing with the optimal parameters is increased to 13.41 Gpa from 7.75 Gpa of the as-deposited film. For only minimizing the surface roughness the two most important laser annealing parameters are laser pulse duration time and pumping frequency. The surface roughness of electroless Ni–P film after laser annealing with the optimal parameters is decreased to 30.84 nm from 110.05 nm of the as-deposited film.

For simultaneously maximizing the film hardness and minimizing the surface roughness, the electroless Ni–P films should be annealed with annealing atmosphere of N_2, laser peak power of 800 W, laser pulse duration time of 0.44 ms, laser pulse frequency of 120 Hz, laser focus height of 10 mm, laser scanning speed of 4 mm/s, scanning line separation of 0.25 mm, and pumping frequency of 20 Hz. The film hardness and the surface roughness of electroless Ni film after laser annealing with these optimal parameters are 11.69 Gpa and 35.22 nm, respectively.

References

[1] Y. Gao, M.Q. Zheng, C.P. Luo, M. Zhu, J. Mater. Res. 23 (2008) 1343.
[2] Y.H. Cheng, Y. Zou, L. Cheng, W. Liu, Mater. Sci. Technol. 24 (2008) 457.

[3] I. Baskaran, T.S.N. Sankara Narayanan, A. Stephen, Mater. Chem. Phys. 99 (2006) 117.
[4] L.W. Liu, S.H. Hsieh, T.K. Tsai, W.J. Chen, S.S. Wu, Thin Solid Films 510 (2006) 102.
[5] G. Lu, G. Li, F. Yu, Wear of Materials, International Conference on Wear of Materials 1985, 1985, p. 382.
[6] T. Osaka, M. Usuda, I. Koiwa, H. Sawai, Jpn. J. Appl. Phys. Part 1 27 (1988) 1885.
[7] N.M. Martyak, S. Wetterer, L. Harrison, M. McNeil, Met. Finish 92 (1994) 111.
[8] H. Ashassi-Sorkhabi, S.H. Rafizadeh, Surf. Coat. Technol. 176 (2003) 318.
[9] R. Taheri, I.N.A. Oguocha, S. Yannacopoulos, Can. Metall. Q. 43 (2004) 363.
[10] I. Apachitei, J. Duszczyk, L. Katgerman, P.J.B. Overkamp, Scripta Mater. 38 (1998) 1347.
[11] M.H. Staia, C. Enriquez, E.S. Puchi, Surf. Coat. Technol. 94–95 (1997) 543.
[12] S.V.S. Tyagi, S.K. Barthwal, V.K. Tondon, S. Ray, Thin Solid Films 169 (1989) 229.
[13] R.S. Razavi, M. Salehi, M. Monirvaghefi, G.R. Gordani, J. Mater. Process. Technol. 195 (2008) 154.
[14] H.H. Shao, X.Y. Jiang, L. Wang, Yinqun Hua, Chin. Opt. Lett. 4 (2006) 589.
[15] K. Matsukawa, M. Katsoka, K. Morinushi, STLE Tribol. Trans. 37 (1994) 573.
[16] M.S. Fernandes de Lima, F.A. Goia, R. Riva, A.M. Espirito Santo, Mater. Res. 10 (2007) 461.
[17] A. Lamikiz, J.A. Sanchez, L.N. Lopez De Lacalle, D. Del Pozo, J.M. Etayo, Mater. Sci. Forum 526 (2006) 217.
[18] H.M. Wang, H.W. Bergmann, Mater. Sci. Eng. 196 (1995) 171.
[19] G. Taguchi, Y. Yokoyama, Y. Wu, Taguchi Methods/Design of Experiments, American Supplier Institute (ASI) Press, Tokyo, Japan, 1993.
[20] I. Haluzan, D. Reichenbach, Circuit World (UK) 17 (4) (1991) 24.
[21] C.Y. Hu, Y.J. Chang, T. Yin, C.Y. Tsao, C.H. Chang, Sens. Actuators B: Chem. 108 (1–2) (2005) 665 (SPEC. ISS.).
[22] S.L. Yim, K.M. Yu, D. Kwok, T.C. Lee, Mater. Sci. Forum 471–472 (2004) 891.
[23] M.R. Chen, International Workshop on Statistical Metrology, Proceedings, IWSM, 1998, p. 96.
[24] J. White, Hybrid Circuit Technol. 8 (5) (1991) 26.
[25] Y.M. Chiang, H. Hsien, Comput. Ind. Eng. 56 (2) (2009) 648.